Mapping the Role of AcrAB-TolC Efflux Pumps in the Evolution of Antibiotic Resistance Reveals Near-MIC Treatments Facilitate Resistance Acquisition

Ariel M. Langevin[a,b], Imane El Meouche[a,b,*], Mary J. Dunlop[a,b,#]

[a] Department of Biomedical Engineering, Boston, Massachusetts, USA

[b] Biological Design Center, Boston, Massachusetts, USA

Running Head: Efflux pumps and resistance evolution

[#] Address correspondence to Mary J. Dunlop, mjdunlop@bu.edu

* Present address: Imane El Meouche, Université de Paris, IAME, UMR1137, INSERM, Paris, France

Word count of Abstract: 246

Word count of Manuscript: 3,508

18 **ABSTRACT**

19 Antibiotic resistance has become a major public health concern as bacteria evolve to evade drugs,
20 leading to recurring infections and a decrease in antibiotic efficacy. Systematic efforts have
21 revealed mechanisms involved in resistance; yet, in many cases, how these specific mechanisms
22 accelerate or slow the evolution of resistance remains unclear. Here, we conducted a systematic
23 study of the impact of the AcrAB-TolC efflux pump on the evolution of antibiotic resistance. We
24 mapped how population growth rate and resistance change over time as a function of both the
25 antibiotic concentration and the parent strain's genetic background. We compared the wild type
26 strain to a strain overexpressing AcrAB-TolC pumps and a strain lacking functional pumps. In all
27 cases, resistance emerged when cultures were treated with chloramphenicol concentrations near
28 the MIC of their respective parent strain. The genetic background of the parent strain also
29 influenced resistance acquisition. The wild type strain evolved resistance within 24 h through
30 mutations in the *acrAB* operon and its associated regulators. Meanwhile, the strain overexpressing
31 AcrAB-TolC evolved resistance more slowly than the wild type strain; this strain achieved
32 resistance in part through point mutations in *acrB* and the *acrAB* promoter. Surprisingly, the strain
33 without functional AcrAB-TolC efflux pumps still gained resistance, which it achieved through
34 upregulation of redundant efflux pumps. Overall, our results suggest that treatment conditions just
35 above the MIC pose the largest risk for the evolution of resistance and that AcrAB-TolC efflux
36 pumps impact the pathway by which chloramphenicol resistance is achieved.

37

38 **IMPORTANCE**

39 Combatting the rise of antibiotic resistance is a significant challenge. Efflux pumps are an
40 important contributor to drug resistance; they exist across many cell types and can export

numerous classes of antibiotics. Cells can regulate pump expression to maintain low intracellular drug concentrations. Here, we explored how resistance emerged depending on the antibiotic concentration, as well as the presence of efflux pumps and their regulators. We found that treatments near antibiotic concentrations that inhibit the parent strain's growth were most likely to promote resistance. While wild type, pump overexpression, and pump knock out strains were all able to evolve resistance, they differed in the absolute level of resistance evolved, the speed at which they achieved resistance, and the genetic pathways involved. These results indicate that specific treatment regimens may be especially problematic for the evolution of resistance and that the strain background can influence how resistance is achieved.

INTRODUCTION

Despite the new wave of antibiotic discovery (1–5), bacteria continue to acquire resistance shortly after the introduction of new drugs for medicinal and industrial applications (6, 7). This is due in large part to the overuse of antibiotics, which results in pressures that drive resistance (8). With limited novel antibiotics and numerous futile antibiotics, doctors and scientists alike are presented with the challenge of how to best treat infections while keeping the evolution of resistance in check.

Adaptive evolution studies have begun exploring how certain antibiotic pressures influence the evolution of resistance. For instance, studies using a 'morbidostat'—a continuous culture device that dynamically adjusts antibiotic concentrations to inhibitory levels—have found numerous targets that can be readily mutated to promote resistance (9–11), as well as identifying how drug switching can limit the evolution of resistance (12). While these studies have provided pivotal

64 insights for this field, the morbidostat design causes antibiotic concentrations to rise to levels that
65 exceed clinically relevant concentrations due to toxicity for patients (13). In recognition of the
66 drug concentration-dependent nature of evolution, researchers have begun to explore bacterial
67 evolution under treatment conditions with lower antibiotic concentrations as well. Wistrand-Yuen
68 *et al.* found that bacteria grown in subinhibitory drug concentractions were still able to achieve
69 high levels of resistance (14–16). Notably, the study identified that the same antibiotic produced
70 unique evolutionary pathways when cells were treated with subinhibitory concentrations as
71 opposed to inhibitory concentrations (14).
72
73 One limitation of current studies within the field is that they can be difficult to compare due to
74 variations in experimental parameters, such as species, antibiotics, or other experimental
75 conditions (17). Given the unique evolutionary pathways at different antibiotic concentrations,
76 systematic mapping of these evolutionary landscapes could provide an improved understanding of
77 which conditions pose the highest risk by allowing direct comparisons between different antibiotic
78 concentrations. For instance, Jahn *et al*. demonstrated that variations in treatment dynamics can
79 significantly alter evolved resistance for some antibiotics, such as tetracycline, but not others, such
80 as amikacin and piperacillin (18). Other evolution experiments that were systematically conducted
81 using a range of concentrations for beta-lactams (19) and erythromycin (20) have highlighted the
82 concentration-dependent adaptability of *Escherichia coli*.
83
84 There are many mechanisms by which antibiotic resistance can be achieved, including enzymatic
85 inactivation, alteration of antibiotic binding sites, and increased efflux or reduced influx of
86 antibiotics (21, 22). Efflux pumps are omnipresent in prokaryotic and eukaryotic cells alike, and

87 are an important contributor to multi-drug resistance (23). AcrAB-TolC in *E. coli* is a canonical
88 example of a multi-drug efflux pump, providing broad-spectrum resistance and raising the MIC of
89 at least nine different classes of antibiotics (24). The pump is composed of three types of proteins:
90 the outer membrane channel protein, TolC; the periplasmic linker protein, AcrA; and the inner
91 membrane protein responsible for substrate recognition and export, AcrB (23). Using the proton
92 motive force, AcrB actively exports antibiotics from the cell (23, 25). The presence of AcrAB-
93 TolC efflux pumps can increase a strain's MIC from ~2-fold to ~10-fold, depending on the
94 antibiotic (26–28). Furthermore, genes associated with these multi-drug resistant efflux pumps,
95 including their local and global regulators, are common targets for mutation as strains evolve high
96 levels of drug resistance (15, 29–32).
97
98 Recent studies have indicated that in addition to providing modest increases in the MIC due to
99 drug export, pumps can also impact mutation rate and evolvability of strains, which may ultimately
100 be more important for the acquisition of high levels of drug resistance. For example, Singh *et al*.
101 found that mutants overexpressing *acrAB* emerged first and afterwards these mutants could evolve
102 high levels of quinolone resistance (33). In addition, heterogeneity in efflux pump expression can
103 predispose subsets of bacterial populations with elevated *acrAB* expression to mutation even prior
104 to antibiotic treatment (34). Deleting genes associated with efflux pumps, such as *tolC*, can also
105 reduce evolvability under antibiotic exposure (35). Further, a recent study in *Staphylococcos*
106 *aureus* found that higher NorA pump levels increased evolvability, and that adding a pump
107 inhibitor could prevent resistance evolution (36). These studies provoke the question of how
108 AcrAB-TolC efflux pumps impact the evolution of drug resistance.
109

110 Our overall goal in this study was to identify how strains with different AcrAB-TolC genotypes
111 evolve antibiotic resistance over time under a range of chloramphenicol concentrations.
112 Chloramphenicol is both a well-validated substrate of AcrAB-TolC and can serve as a last resort
113 antibiotic in multi-drug resistant infections, as most clinical isolates are still susceptible to this
114 drug (37, 38). To identify how AcrAB-TolC impacts the evolution of resistance, we used a
115 turbidostat as an evolutionary platform (39) and measured changes in fitness and resistance. We
116 evolved three strains with different levels of AcrAB-TolC: a wild type strain with the native
117 regulatory network controlling AcrAB-TolC expression (WT); a strain which lacks the local
118 regulator AcrR (AcrAB+), which results in a 1.5 to 6-fold increase in expression of the pumps
119 (40–42); and a strain lacking functional AcrAB-TolC efflux pumps (Δ*acrB*). We allowed the
120 cultures to grow and evolve for 72 h in continuous culture while continuously recording growth
121 rates. We periodically sampled the cultures and assessed the population's resistance. We then
122 charted the evolutionary landscapes for each of the three strains under different chloramphenicol
123 concentrations to identify which circumstances gave rise to resistance.
124
125 **RESULTS**
126 In order to systematically evaluate the evolutionary landscape of efflux pump-mediated antibiotic
127 resistance, we used the eVOLVER, a modular turbidostat capable of growing independent cultures
128 in parallel (39). This platform allowed us to track a culture's fitness by measuring growth rate
129 continuously over multi-day experiments. In addition to this, we collected samples at selected
130 intervals and, with these samples, performed antibiotic disc diffusion assays to assess the
131 population's resistance and spot assays to quantify the presences of high-resistance isolates within
132 the population (Figure 1).

133

134 We mapped growth rates over time for cultures subjected to a range of chloramphenicol treatment
135 concentrations (Figure 2A & Figure S1). To compare across strains, we defined MIC^0_{parent} as the
136 MIC of the parent strain (MIC^0_{WT} = 2 µg/mL, MIC^0_{AcrAB+} = 2 µg/mL, $MIC^0_{\Delta acrB}$ = 0.5 µg/mL). We
137 found similar values for MIC^0_{WT} and MIC^0_{AcrAB+} (Figure S2), which may be due to induction of
138 efflux pump expression in the WT strain in the presence of chloramphenicol. Prior studies have
139 shown that the presence of stress can increase pump expression by 4-fold (40, 43), which is
140 comparable to the impact of deleting *acrR* (40–42). We found that treatment with high
141 concentrations of chloramphenicol repressed bacterial growth for multiple days. We observed this
142 growth inhibition at ~10 µg/mL for WT and AcrAB+, and at ~2 µg/mL for Δ*acrB*. These inhibitory
143 concentrations represent treatments of ~5x MIC^0_{parent} for all three strains. We found that cultures
144 grown in lower chloramphenicol concentrations were able to recover growth. For example, when
145 we treated cultures with ~1-2x MIC^0_{parent}, we observed a significant decrease in the growth rate
146 between 0 and 12 h (Table S1). However, after 12 to 24 h, growth in these populations was partially
147 restored. At lower treatment concentrations (<1x MIC^0_{parent}), all cultures were able to grow, though
148 usually at a deficit compared to the 0 µg/mL chloramphenicol condition. For all three strains, there
149 were qualitatively similar growth recovery patterns, with an initial growth repression phase
150 followed by a partially restored growth phase (Figure S1).

151

152 The growth rate results suggested the evolution of drug resistance within the population (9, 18).
153 To quantify this, we used an antibiotic disc assay to map the corresponding resistance levels
154 (Figure 2B & Figure S3). We found distinct increases in resistance levels that corresponded to
155 populations which recovered growth. While there were qualitative similarities for the three strains,

156 the timing and level of resistance achieved was dependent on the strain background. We classified
157 populations as resistant when their inhibition zone diameters were smaller than 12 mm, following
158 established standards for antimicrobial susceptibility testing (44). The WT strain gained resistance
159 under a broad range of chloramphenicol treatment concentrations; this resistance emerged within
160 24 h when cells were treated with ~1-2x MIC^0_{WT}. The AcrAB+ strain, where efflux pumps are
161 overexpressed, was able to evolve resistance as well, albeit at a slower rate and at lower levels than
162 WT. AcrAB+ achieved resistance within 48 h when treated with 2.5x MIC^0_{AcrAB+}, but the range of
163 chloramphenicol concentrations that resulted in resistance was narrower than for the WT strain.
164 The Δ*acrB* cells achieved resistance more slowly, but for the range of ~1-2x $MIC^0_{\Delta acrB}$
165 chloramphenicol cultures were still able to reach resistant levels (Figure 2B & Figure S3).
166
167 To compare the ultimate evolved resistance levels, we calculated the final, absolute MIC of the
168 populations at 72 h. When we normalized the treatment concentration by MIC^0_{parent}, we found that
169 treatments concentrations ~1-2x MIC^0_{parent} evolved the most resistant populations (Figure 2C).
170 Selective pressures of subinhibitory antibiotic concentrations have often been considered high-risk
171 for the evolution of resistance (14, 45). Yet, our results indicated that concentrations near or just
172 above MIC^0_{parent} lead to the highest resistance levels in these conditions. In short, all three strains
173 were able to evolve resistance when treated with ~1-2x MIC^0_{parent} chloramphenicol, with WT
174 achieving the highest final, absolute MIC of the three strains. WT evolved more rapidly than
175 AcrAB+ or Δ*acrB*. Moreover, the relative range of chloramphenicol concentrations that supported
176 the evolution of resistance in the AcrAB+ strain was narrower than for WT or Δ*acrB* strains.
177

178 We next asked how resistance and growth changed through time. We found that in the absence of
179 antibiotics, the trajectories trended largely towards faster growth, with minimal changes to
180 resistance levels (Figure 3). With subinhibitory chloramphenicol treatments, we observed that the
181 populations first experienced a slight growth decrease, followed by increased resistance, and then
182 restored growth within 48 h. While these populations did gain resistance, they did not tend to reach
183 very high final MIC values in absolute terms, with inhibition zone diameters just at the border of
184 being defined as resistant. In contrast, with inhibitory chloramphenicol treatment, there was a more
185 dramatic reduction in growth within the first 12 h. Though growth was impacted, the populations
186 tended to walk towards high resistance during this period. As depicted in the schematics, the zig-
187 zag patterns trending towards high resistance may be indicative of the cultures acquiring resistant
188 mutations and compensating for the associated fitness costs of these mutations. Finally, at high
189 chloramphenicol concentrations, bacteria first became more susceptible and then stopped growing
190 entirely within 12 h; growth was never restored for these populations. We found that all strains
191 followed similar evolutionary trajectories while balancing the trade-off between growth and
192 resistance. These findings highlight the importance of using antibiotic concentrations that are
193 sufficiently inhibitory.
194
195 While these results tell us about the growth rate and resistance of the overall population, it is
196 difficult to determine if sub-populations of cells within the culture have acquired high levels of
197 resistance from disc assays alone. First, because the disc assays do not quantify resistance
198 associated with individual cells in the culture, they cannot reveal the presence of subpopulations
199 of resistant and susceptible cells. Second, beyond a certain resistance level, cells will grow up to
200 the boundary of the disc; thus, it is not possible to quantify resistance increases beyond this.

201 Determining which conditions can give rise to high levels of resistance is important for revealing
202 particularly dangerous treatment regimes. In addition, sub-populations with increased resistance
203 to one antibiotic can promote cross-resistance to other drugs (45).
204
205 To quantify the fraction of resistant cells that emerged during our evolution experiment, we
206 conducted a spot assay, in which we measured the fraction of the population capable of surviving
207 on specific chloramphenicol concentrations. For all three strains, we observed sub-populations that
208 were capable of growing on 10 μg/mL chloramphenicol (Figure 4A & Figure S4). Interestingly,
209 these cells primarily emerged from treatment conditions with lower levels of chloramphenicol, and
210 not from conditions where cells were subjected to 10 μg/mL chloramphenicol. For example, at
211 least 0.1% of the population from each of the three WT replicates that were treated at 2 μg/mL
212 chloramphenicol could survive on 10 μg/mL at the end of the experiment. We did find cases where
213 WT cells treated with 10 μg/mL evolved resistance to 10 μg/mL, however this was less common
214 than in lower treatment concentrations. Thus, cultures were able to evolve resistance to higher
215 levels of chloramphenicol than they were subjected to, a feature that was most pronounced when
216 treatments were just above or at MIC^0_{WT}. These results closely match trends in the population's
217 overall resistance (Figure 2B). We also found isolates capable of growing on 20 μg/mL
218 chloramphenicol, with a reduced frequency relative to 10 μg/mL (Figure 4B & Figure S4).
219
220 In contrast, the AcrAB+ strain was capable of evolving resistance to 10 μg/mL when treated with
221 5 μg/mL chloramphenicol; yet, surprisingly, AcrAB+ never produced a sub-population that was
222 able to grow on 20 μg/mL as the WT did. Meanwhile, despite the higher initial susceptibility of
223 Δ*acrB* ($MIC^0_{\Delta acrB} < MIC^0_{WT}$ and MIC^0_{AcrAB+}), the Δ*acrB* strain consistently produced sub-

224 populations that were able to grow at 20 µg/mL chloramphenicol by 72 h. This sub-population
225 appeared for chloramphenicol concentrations around 2 µg/mL, similar to the WT strain.
226
227 A key question remained: which mutations were responsible for the increases in resistance we
228 observed? To address this, we used whole genome sequencing to analyze three biological
229 replicates from the 72 h timepoint for the WT, AcrAB+, and Δ*acrB* strains (Table S2). For the WT
230 strain, each of the sequenced isolates contained a single point mutation in the DNA binding region
231 of *marR*, which can upregulate AcrAB-TolC efflux pumps and expression of other stress response
232 genes (46). Two of these point mutations were missense mutations in *marR* and have been
233 observed in other studies (47–51). Additionally, one isolate had a missense mutation in the
234 periplasmic encoding region of *acrB*. The other two isolates had an IS1 or IS5 insertional sequence
235 interrupting *acrR*, which is known to upregulate *acrAB* (52). One question these results raise is
236 why the AcrAB+ strain, where *acrR* is removed, is outperformed by WT strains with mutations in
237 *acrR*. A potential explanation for this is that the 'marbox' through which *acrAB* is upregulated sits
238 within *acrR* (53). The AcrAB+ strain lacks this marbox (54), while in the sequenced isolates the
239 insertion sequence is located further upstream in *acrR* and the marbox remains intact, providing
240 global stress response regulation while eliminating the impact of the local repressor. Thus, the
241 exact position of the insertion sequence matters. These sequencing results indicate that strains
242 containing AcrAB-TolC efflux pumps use mutations related to the pumps and their regulation to
243 optimize survival and increase resistance in the presence of chloramphenicol.
244
245 When we evolved the AcrAB+ strain and performed whole genome sequencing of the most
246 resistant isolates, all isolates had mutations in the noncoding, promoter region of *acrAB* (Table

247 S2). These mutations indicate that the AcrAB+ strain might require further tuning of *acrAB*
248 expression for improved resistance. Further, two of these isolates also had missense mutations in
249 the coding region of *acrB* as well. Of these, the V139F missense mutation is known to produce
250 high levels of multidrug resistance by accelerating export for a number of AcrAB-TolC substrates
251 (11, 18, 55, 56). We observed *acrB* Q569L evolve from two different parent strains, WT and
252 AcrAB+, suggesting it plays a role in chloramphenicol export. Additionally, the evolved AcrAB+
253 isolates all had other mutations less directly related to the AcrAB-TolC efflux pump and its
254 regulators, such as genes related to transcription (*rpoB*, *yhjB*), fimbriae assembly (*fimD*), or
255 degradation (*clpX*) (Table S2).
256
257 In contrast, when we evolved the Δ*acrB* strain, we found that all three isolates had an insertion
258 sequence located in *acrS* (Table S2). AcrS is the local regulator of the AcrEF-TolC efflux pump,
259 a homolog to AcrAB-TolC (57). This result agrees with findings from Cudkowicz & Schuldiner,
260 who showed that the Δ*acrB* strain gained high resistance by upregulating redundant efflux pumps
261 in *E. coli*, such as AcrEF-TolC or MdtEF-TolC (11). One of the three isolates also contained a
262 missense mutation in the tRNA for selenocysteine (*selA*) and a short insertion sequence in the 16S
263 rRNA of the 30S subunit (*rrsG*), though whether or how these play a role in chloramphenicol
264 resistance is unclear.
265
266 **DISCUSSION**
267 In this work, we identified that treating strains with antibiotic concentrations close to MIC^0_{parent}
268 promotes the evolution of resistance; however, the evolvability and ultimate resistance level
269 achieved differed between WT, AcrAB+, and Δ*acrB* strains. WT populations evolved mutations

270 that conferred high levels of resistance within 24 h after antibiotic exposure. Maximal resistance
271 was evolved at ~1x MIC^0_{WT}, however 0.25-2.5x MIC^0_{WT} chloramphenicol treatment
272 concentrations all gave rise to resistance. In contrast, AcrAB+ evolved resistance, but this was
273 only possible at precise chloramphenicol concentrations at 2.5x MIC^0_{AcrAB+}. The evolved AcrAB+
274 populations were less resistant than their WT counterparts, and spot assays determining resistance
275 confirmed this trend. In contrast, the Δ*acrB* strain was able to evolve resistance under 1-4x
276 $MIC^0_{\Delta acrB}$ chloramphenicol treatments, and ultimately achieved absolute resistance levels
277 comparable to those observed in the WT strain.
278
279 Our results identify that antibiotic treatments near MIC^0_{parent} are especially prone to evolving
280 resistance. Reding *et al*. observed this hotspot for adaptability of *E. coli* in the presence of another
281 antibiotic, erythromycin, just below the MIC of their parent strains (20). While doctors measure
282 resistance of bacterial infections, they sometimes prescribe antibiotic treatment prior to obtaining
283 the results of this assay (58) or use a treatment concentration too low to effectively penetrate the
284 infection site (59). This blind treatment could lead to increased levels of resistance (60, 61). These
285 results highlight the presence of regimes that are especially problematic and which should be
286 avoided to limit the evolution of antibiotic resistance.
287
288 While we observed that all strains were capable of evolving resistance, sequencing revealed the
289 different pathways that each strain took to achieve this. WT achieved resistance through mutations
290 and insertion sequences in the regulators AcrR and MarR, suggesting that WT cells can fine-tune
291 expression of the AcrAB-TolC pumps to gain resistance to chloramphenicol. Interestingly, these
292 mutations may produce cross-resistance to other antibiotics as well since these regulators control

293 many genes involved in multi-drug resistance (62, 63). AcrAB+ cells utilized mutations in *acrB*
294 and the promoter region controlling its expression to achieve resistance. Δ*acrB* populations
295 achieved resistance by targeting homologous efflux pump systems, such as AcrEF-TolC. Although
296 resistance was slow to emerge in this strain compared to WT or AcrAB+, this alternative pathway
297 for achieving resistance ultimately resulted in levels comparable to those achieved by the WT
298 strain. By charting evolutionary landscapes across different antibiotic concentrations, we have
299 gained insight into treatments that impact the emergence of antibiotic resistance and the effect of
300 efflux pumps on this process.
301
302 **METHODS**
303 **Bacterial Strains**
304 We used *E. coli* strains BW25113 (WT), BW25113 Δ*acrR* (AcrAB+), and BW25113 Δ*acrB*
305 (Δ*acrB*) as the parent strains. The WT strain BW25113 is the base strain for the Keio collection
306 (54). For BW25113 Δ*acrR*, we designed primers with homology regions on *acrR* and amplified
307 the kanamycin resistance marker and FRT sites of pKD13 (54). Primers are listed in Table S3. The
308 linear DNA was then treated using a DpnI digest and PCR purification. We electroporated the
309 purified linear DNA into competent BW25113 cells containing the plasmid pSIM6 (64). BW25113
310 Δ*acrB* was derived from Keio collection strain JW0451 (BW25113 Δ*acrB*::kan^R) (26). We
311 removed kanamycin resistance markers from BW25113 Δ*acrR*::kan^R and JW0451 following the
312 pCP20 protocol from Reference (65).
313
314 **Determination of MIC**

315 For all experiments, overnight cultures were inoculated from a single colony in 10 mL LB and
316 grown in a 50 mL Erlenmeyer flask at 37°C with 200 rpm orbital shaking. After overnight growth,
317 the optical density at 600 nm (OD_{600}) was measured, and the initial volume was diluted back to
318 OD_{600} = 0.1. To determine the MIC of the parent strains (Figure S2), we added a final concentration
319 of 0, 0.2, 0.5, 1, 2, 4, 8, or 12 µg/mL chloramphenicol to each culture; to determine the MIC of the
320 evolved strains (Figure S5), we added 0, 0.5, 1, 2, 5, 10, 20, or 50 µg/mL to each culture.
321 Chloramphenicol stocks were prepared with 100% ethanol. The samples were sealed with
322 evaporation-limiting membranes (Thermo Scientific AB-0580) and grown in 24-well plates at
323 37°C with 200 rpm orbital shaking. OD_{600} readings were taken using a BioTek Synergy H1m plate
324 reader before incubation (t = 0 h) and after antibiotic exposure (t = 24 h). All experiments were
325 performed in triplicate using biological replicates.
326
327 **Experimental Conditions in the eVOLVER**
328 In the eVOLVER, cultures were inoculated from a single colony in LB at 37°C. A stir bar mixed
329 the cultures on a medium setting, or approximately 1000 rpm (39). The LB was supplemented with
330 the detergent Tween20 (Sigma Aldrich Cat. # P1379) at 0.2% (v/v) to reduce spurious OD_{600}
331 measurements caused by biofilm growth on the flask. As Tween20 is a detergent and a potential
332 substrate of the AcrAB-TolC efflux pumps, we also conducted the toxicity curve experiments with
333 Tween20 at our working concentration 0.2% (v/v). We found there was no significant change in
334 resistance for any of the strains in the presence of Tween20 (Figure S6 & Table S4).
335
336 Cells were inoculated in the eVOLVER overnight (t ≈ -16 – -14 h) prior to the beginning of the
337 experiment (t = 0 h) to establish steady-state exponential growth. We set the eVOLVER using an

338 upper OD_{600} bound of 0.2 and a lower bound of 0.1; thus, cultures were grown to a turbidity of 0.2
339 and then diluted back to 0.1 to maintain the turbidostat at approximately constant cell density.
340 Samples were collected during the experiment at set time points (t = 0, 1, 3, 6, 12, 24, 48, and 72
341 h) and used for downstream analysis. All experiments were performed in triplicate using biological
342 replicates.
343
344 At t = 0 h, we introduced chloramphenicol at a predetermined final treatment concentration (0, 0.2,
345 0.5, 1, 2, 5, 10, or 20 µg/mL). This introduction was implemented by switching the media source
346 from one containing 0 µg/mL chloramphenicol to another containing the final treatment
347 concentration; in addition, we spiked the samples directly with the treatment concentration of
348 chloramphenicol at the same time to avoid a delay due to the time required for media cycling in
349 the turbidostat.
350
351 **Downstream Assays and Data Collection from eVOLVER Samples**
352 Growth Rate Measurements
353 Growth rate measurements were calculated after each dilution event using:

354 $$\text{Growth Rate} = \frac{\ln\left(\frac{OD_{600,high}}{OD_{600,low}}\right)}{t_{OD_{600,high}} - t_{OD_{600,low}}}$$

355 The growth rate between each dilution was then averaged across sampling time points to compare
356 against disc diffusion assays and spot assays. For example, the growth rate given at t = 0 h is the
357 growth rate from t = -6 h to t = 0 h. To evaluate statistically significant differences in growth rate
358 between two time points, we used the paired-*t* test; to evaluate statistically significant differences
359 in growth rate between two strains, we used the *t* test (Table S1A).

360

361 Antibiotic Disc Diffusion Assay

362 We aliquoted samples from the eVOLVER, where the OD_{600} from each sample was between 0.1
363 and 0.2. We used cotton swabs to cover LB agar plates with a layer of the sample (66). An
364 antibiotic disc containing chloramphenicol (30 g) (Thermo Fisher Scientific Cat. # CT0013B) was
365 then placed on the plate. The plate was incubated for 24 h at 37°C. The diameter of the zone of
366 inhibition around each disc was then measured. Diameter of inhibition zones were classified as
367 susceptible, intermediate, or resistant based on Reference (44). Additionally, we calculated the
368 MIC using a mapping between MIC and diameter of inhibition zones for our samples (Figure S5)
369 (67). To evaluate statistically significant differences in diameter of inhibition zones or resistance
370 between two time points, we used the paired-*t* test; to evaluate statistically significant differences
371 in resistance between two genotypes, we used the *t* test (Table S1B).

372

373 Spot Assay

374 The samples from the eVOLVER experiment were diluted in PBS in the following dilution series:
375 1, 10^{-1}, 10^{-2}, 10^{-3}, 10^{-4}, and 10^{-5}. We then plated 2.5 µL of each dilution on LB agar plates
376 containing 0, 0.5, 1, 2, 5, 10, and 20 µg/mL chloramphenicol. The plates were then incubated for
377 24 h at 37°C. To count colonies, we identified the dilution factor with the most countable colonies,
378 and recorded the number of colony forming units (*CFU*) and dilution factor (*d*). The CFU/mL for
379 each sample was then calculated by:

380 $$\text{CFU/mL} = \frac{CFU * d}{V}$$

381 where V is the volume plated. We also calculated the proportion of the population able to grow on
382 different concentrations of chloramphenicol by calculating the CFU/mL from LB agar plates
383 containing 0, 0.5, 1, 2, 5, 10, and 20 µg/mL chloramphenicol.
384
385 **Whole Genome Sequencing**
386 DNA was extracted from single isolates and parent strains using the QIAGEN DNeasy
387 PowerBiofilm kit. For each strain, we selected three isolates to sequence; each of these isolates
388 originated from a different biological replicate that was evolved under the same experimental
389 conditions (i.e. each isolate comes from a different eVOLVER culture). Samples were sequenced
390 at the Microbial Genome Sequencing Center (MiGS) in Pittsburg, PA, USA, who conducted
391 library preparation and multiplexing using the Illumina Nextera kit series and then sequenced using
392 a NextSeq 550 platform with 150 bp paired-ends and an average coverage of 50 reads. We
393 analyzed reads using *breseq* (68) version 0.35.1. Reads were aligned to the BW25113 Keio
394 reference genome (Accession no.: CP009273) in consensus mode. The treatment concentrations
395 and isolation concentrations used to select each isolate are listed in Table S2.
396
397 **Data Availability**
398 Whole genome sequencing data for the parent strains and the isolates are available on GenBank
399 (BioProject: PRJNA666010; Accession no.: CP062239 to CP062250). Other datasets generated
400 during this study are available from the corresponding author upon request.
401
402 **ACKNOWLEDGEMENTS**

403 This research was supported by the National Science Foundation (grant No. 1347635) and the
404 National Institutes of Health (grant No. R01AI102922).
405
406 We thank Dr. Mo Khalil, Dr. Brandon Wong, Dr. Chris Mancuso, and Zack Heins for their
407 assistance and support with the eVOLVER.
408

409 **REFERENCES**

410 1. Smith PA, Koehler MFT, Girgis HS, Yan D, Chen Y, Chen Y, Crawford JJ, Durk MR,
411 Higuchi RI, Kang J, Murray J, Paraselli P, Park S, Phung W, Quinn JG, Roberts TC,
412 Rougé L, Schwarz JB, Skippington E, Wai J, Xu M, Yu Z, Zhang H, Tan MW, Heise CE.
413 2018. Optimized arylomycins are a new class of Gram-negative antibiotics. Nature
414 561:189–194.
415 2. Sousa MC. 2019. New antibiotics target the outer membrane of bacteria. Nature. NLM
416 (Medline).
417 3. Imai Y, Meyer KJ, Iinishi A, Favre-Godal Q, Green R, Manuse S, Caboni M, Mori M,
418 Niles S, Ghiglieri M, Honrao C, Ma X, Guo JJ, Makriyannis A, Linares-Otoya L,
419 Böhringer N, Wuisan ZG, Kaur H, Wu R, Mateus A, Typas A, Savitski MM, Espinoza JL,
420 O'Rourke A, Nelson KE, Hiller S, Noinaj N, Schäberle TF, D'Onofrio A, Lewis K. 2019.
421 A new antibiotic selectively kills Gram-negative pathogens. Nature 576:459–464.
422 4. Hart EM, Mitchell AM, Konovalova A, Grabowicz M, Sheng J, Han X, Rodriguez-Rivera
423 FP, Schwaid AG, Malinverni JC, Balibar CJ, Bodea S, Si Q, Wang H, Homsher MF,
424 Painter RE, Ogawa AK, Sutterlin H, Roemer T, Black TA, Rothman DM, Walker SS,
425 Silhavy TJ. 2019. A small-molecule inhibitor of BamA impervious to efflux and the outer

426 membrane permeability barrier. Proc Natl Acad Sci U S A 116:21748–21757.
427 5. Luther A, Urfer M, Zahn M, Müller M, Wang SY, Mondal M, Vitale A, Hartmann JB,
428 Sharpe T, Monte F Lo, Kocherla H, Cline E, Pessi G, Rath P, Modaresi SM, Chiquet P,
429 Stiegeler S, Verbree C, Remus T, Schmitt M, Kolopp C, Westwood MA, Desjonquères N,
430 Brabet E, Hell S, LePoupon K, Vermeulen A, Jaisson R, Rithié V, Upert G, Lederer A,
431 Zbinden P, Wach A, Moehle K, Zerbe K, Locher HH, Bernardini F, Dale GE, Eberl L,
432 Wollscheid B, Hiller S, Robinson JA, Obrecht D. 2019. Chimeric peptidomimetic
433 antibiotics against Gram-negative bacteria. Nature 576:452–458.
434 6. Davies J, Davies D. 2010. Origins and Evolution of Antibiotic Resistance. Microbiol Mol
435 Biol Rev 74:417–433.
436 7. England PH. 2015. Health Matter – tackling antimicrobial resistance. GOVUK.
437 8. Ventola CL. 2015. The Antibiotic Resistance Crisis: Part 1: Causes and Threats. Pharm
438 Ther 40:277–283.
439 9. Toprak E, Veres A, Yildiz S, Pedraza JM, Chait R, Paulsson J, Kishony R. 2013. Building
440 a morbidostat: An automated continuous-culture device for studying bacterial drug
441 resistance under dynamically sustained drug inhibition. Nat Protoc 8:555–567.
442 10. Toprak E, Veres A, Michel J-B, Chait R, Hartl DL, Kishony R. 2011. Evolutionary paths
443 to antibiotic resistance under dynamically sustained drug selection. Nat Genet 44:101.
444 11. Alon Cudkowicz N, Schuldiner S. 2019. Deletion of the major *Escherichia coli* multidrug
445 transporter AcrB reveals transporter plasticity and redundancy in bacterial cells. PLoS
446 One 14:e0218828.
447 12. Yoshida M, Reyes SG, Tsuda S, Horinouchi T, Furusawa C, Cronin L. 2017. Time-
448 programmable drug dosing allows the manipulation, suppression and reversal of antibiotic

449 drug resistance *in vitro*. Nat Commun 8:1–11.

450 13. Marchant J. 2018. When antibiotics turn toxic. Nature 555:431–433.

451 14. Wistrand-Yuen E, Knopp M, Hjort K, Koskiniemi S, Berg OG, Andersson DI. 2018.
452 Evolution of high-level resistance during low-level antibiotic exposure. Nat Commun
453 9:1599.

454 15. Kohanski MA, DePristo MA, Collins JJ. 2010. Sublethal Antibiotic Treatment Leads to
455 Multidrug Resistance via Radical-Induced Mutagenesis. Mol Cell 37:311–320.

456 16. Andersson DI, Hughes D. 2012. Evolution of antibiotic resistance at non-lethal drug
457 concentrations. Drug Resist Updat 15:162–172.

458 17. Strauss SK, Schirman D, Jona G, Brooks AN, Kunjapur AM, Nguyen Ba AN, Flint A,
459 Solt A, Mershin A, Dixit A, Yona AH, Csörgő B, Busby BP, Hennig BP, Pál C,
460 Schraivogel D, Schultz D, Wernick DG, Agashe D, Levi D, Zabezhinsky D, Russ D, Sass
461 E, Tamar E, Herz E, Levy ED, Church GM, Yelin I, Nachman I, Gerst JE, Georgeson JM,
462 Adamala KP, Steinmetz LM, Rübsam M, Ralser M, Klutstein M, Desai MM, Walunjkar
463 N, Yin N, Hefetz NA, Jakimo N, Snitser O, Adini O, Kumar P, Smith RSH, Zean R,
464 Hazan R, Rak R, Kishony R, Johnson S, Nouriel S, Vonesch SC, Foster S, Dagan T, Wein
465 T, Karydis T, Wannier TM, Stiles T, Olin-Sandoval V, Mueller WF, Bar-On YM, Dahan
466 O, Pilpel Y. 2019. Evolthon: A community endeavor to evolve lab evolution. PLoS Biol
467 17(3):e3000182.

468 18. Jahn LJ, Munck C, Ellabaan MMH, Sommer MOA. 2017. Adaptive Laboratory Evolution
469 of Antibiotic Resistance Using Different Selection Regimes Lead to Similar Phenotypes
470 and Genotypes. Front Microbiol 8:816.

471 19. Russ D, Glaser F, Shaer Tamar E, Yelin I, Baym M, Kelsic ED, Zampaloni C, Haldimann

472 A, Kishony R. 2020. Escape mutations circumvent a tradeoff between resistance to a beta-
473 lactam and resistance to a beta-lactamase inhibitor. Nat Commun 11:1–9.
474 20. Reding C, Catalán P, Jansen G, Bergmiller T, Rosenstiel P, Schulenburg H, Gudelj I,
475 Beardmore R. 2019. Hotspot Dosages of Most Rapid Antibiotic Resistance Evolution.
476 bioRxiv 866269.
477 21. Delcour AH. 2009. Outer Membrane Permeability and Antibiotic Resistance. Biochim
478 Biophys Acta 1794:808–816.
479 22. Blair JMA, Webber MA, Baylay AJ, Ogbolu DO, Piddock LJ V. 2015. Molecular
480 mechanisms of antibiotic resistance. Nat Rev Micro 13:42–51.
481 23. Li X-Z, Plésiat P, Nikaido H. 2015. The Challenge of Efflux-Mediated Antibiotic
482 Resistance in Gram-Negative Bacteria. Clin Microbiol Rev 28:337–418.
483 24. Kobylka J, Kuth MS, Müller RT, Geertsma ER, Pos KM. 2020. AcrB: a mean, keen, drug
484 efflux machine. Ann N Y Acad Sci 1459:38–68.
485 25. Nikaido H, Takatsuka Y. 2009. Mechanisms of RND Multidrug Efflux Pumps. Biochim
486 Biophys Acta 1794:769–781.
487 26. Langevin AM, Dunlop MJ. 2018. Stress introduction rate alters the benefit of AcrAB-
488 TolC efflux pumps. J Bacteriol 200.
489 27. Okusu H, Ma D, Nikaido H. 1996. AcrAB efflux pump plays a major role in the antibiotic
490 resistance phenotype of *Escherichia coli* multiple-antibiotic-resistance (Mar) mutants. J
491 Bacteriol 178:306–308.
492 28. Zwama M, Yamasaki S, Nakashima R, Sakurai K, Nishino K, Yamaguchi A. 2018.
493 Multiple entry pathways within the efflux transporter AcrB contribute to multidrug
494 recognition. Nat Commun 9:1–9.

495 29. Webber MA, Talukder A, Piddock LJV. 2005. Contribution of mutation at amino acid 45
496 of AcrR to *acrB* expression and ciprofloxacin resistance in clinical and veterinary
497 *Escherichia coli* isolates. Antimicrob Agents Chemother 49:4390–4392.
498 30. Olliver A, Vallé M, Chaslus-Dancla E, Cloeckaert A. 2004. Role of an *acrR* mutation in
499 multidrug resistance of *in vitro*-selected fluoroquinolone-resistant mutants of *Salmonella*
500 *enterica* serovar Typhimurium. FEMS Microbiol Lett 238:267–272.
501 31. Wang H, Dzink-Fox JL, Chen M, Levy SB. 2001. Genetic characterization of highly
502 fluoroquinolone-resistant clinical *Escherichia coli* strains from China: Role of *acrR*
503 mutations. Antimicrob Agents Chemother 45:1515–1521.
504 32. Baym M, Lieberman TD, Kelsic ED, Chait R, Gross R, Yelin I, Kishony R. 2016.
505 Spatiotemporal microbial evolution on antibiotic landscapes. Science 353:1147–1151.
506 33. Singh R, Swick MC, Ledesma KR, Yang Z, Hu M, Zechiedrich L, Tama VH. 2012.
507 Temporal interplay between efflux pumps and target mutations in development of
508 antibiotic resistance in Escherichia coli. Antimicrob Agents Chemother 56:1680–1685.
509 34. El Meouche I, Dunlop MJ. 2018. Heterogeneity in efflux pump expression predisposes
510 antibiotic-resistant cells to mutation. Science 362:686 LP – 690.
511 35. Lukačišinová M, Fernando B, Bollenbach T. 2020. Highly parallel lab evolution reveals
512 that epistasis can curb the evolution of antibiotic resistance. Nat Commun 11:3105.
513 36. Papkou A, Hedge J, Kapel N, Young B, MacLean RC. 2020. Efflux pump activity
514 potentiates the evolution of antibiotic resistance across S. aureus isolates. Nat Commun
515 11:1–15.
516 37. Sood S. 2016. Chloramphenicol - A Potent Armament Against Multi-Drug Resistant
517 (MDR) Gram Negative Bacilli? J Clin Diagn Res2016/02/01. 10:DC01-DC3.

518 38. Nitzan O, Kennes Y, Colodner R, Saliba W, EdelsteinI H, Raz R, Chazan B. 2015.
519 Chloramphenicol use and susceptibility patterns in Israel: a national survey. Isr Med
520 Assoc J 17:27–31.
521 39. Wong BG, Mancuso CP, Kiriakov S, Bashor CJ, Khalil AS. 2018. Precise, automated
522 control of conditions for high-throughput growth of yeast and bacteria with eVOLVER.
523 Nat Biotechnol 36:614.
524 40. Ruiz C, Levy SB. 2014. Regulation of *acrAB* expression by cellular metabolites in
525 *Escherichia coli*. J Antimicrob Chemother 69:390–399.
526 41. Luhe AL, Gerken H, Tan L, Wu J, Zhao H. 2012. Alcohol tolerance of Escherichia coli
527 acrR and marR regulatory mutants. J Mol Catal B Enzym 76:89–93.
528 42. Subhadra B, Kim J, Kim DH, Woo K, Oh MH, Choi CH. 2018. Local repressor AcrR
529 regulates AcrAB efflux pump required for biofilm formation and virulence in
530 Acinetobacter nosocomialis. Front Cell Infect Microbiol 8:270.
531 43. Chetri S, Bhowmik D, Paul D, Pandey P, Chanda DD, Chakravarty A, Bora D,
532 Bhattacharjee A. 2019. AcrAB-TolC efflux pump system plays a role in carbapenem non-
533 susceptibility in Escherichia coli. BMC Microbiol 19:210.
534 44. Clinical and Laboratory Standards Institute. 2013. M100-S23 Performance Standards for
535 Antimicrobial Susceptibility Testing; Twenty-Third Informational Supplement, 33rd ed.
536 Wayne, PA.
537 45. Andersson DI, Balaban NQ, Baquero F, Courvalin P, Glaser P, Gophna U, Kishony R,
538 Molin S, Tønjum T. 2020. Antibiotic resistance: turning evolutionary principles into
539 clinical reality. FEMS Microbiol Rev.
540 46. McMurry LM, Levy SB. 2013. Amino acid residues involved in inactivation of the

541 *Escherichia coli* multidrug resistance repressor MarR by salicylate, 2,4-dinitrophenol, and
542 plumbagin. FEMS Microbiol Lett 349(1):16–24.
543 47. Linkevicius M, Sandegren L, Andersson DI. 2013. Mechanisms and fitness costs of
544 tigecycline resistance in escherichia coli. J Antimicrob Chemother 68:2809–2819.
545 48. Lu J, Jin M, Nguyen SH, Mao L, Li J, Coin LJM, Yuan Z, Guo J. 2018. Non-antibiotic
546 antimicrobial triclosan induces multiple antibiotic resistance through genetic mutation.
547 Environ Int 118:257–265.
548 49. Ching C, Zaman MH. 2020. Development and selection of low-level multi-drug resistance
549 over an extended range of sub-inhibitory ciprofloxacin concentrations in Escherichia coli.
550 Sci Rep 10:1–9.
551 50. Lázár V, Kishony R. 2019. Transient antibiotic resistance calls for attention. Nat
552 Microbiol 4:1606–1607.
553 51. Hickman RA, Munck C, Sommer MOA. 2017. Time-Resolved Tracking of Mutations
554 Reveals Diverse Allele Dynamics during Escherichia coli Antimicrobial Adaptive
555 Evolution to Single Drugs and Drug Pairs. Front Microbiol 8:893.
556 52. Grenier F, Matteau D, Baby V, Rodrigue S. 2014. Complete genome sequence of
557 *Escherichia coli* BW25113. Genome Announc 2(5):e01038-14.
558 53. Watanabe R, Doukyu N. 2012. Contributions of mutations in acrR and marR genes to
559 organic solvent tolerance in Escherichia coli. AMB Express 2:1–11.
560 54. Baba T, Ara T, Hasegawa M, Takai Y, Okumura Y, Baba M, Datsenko KA, Tomita M,
561 Wanner BL, Mori H. 2006. Construction of *Escherichia coli* K-12 in-frame, single-gene
562 knockout mutants: the Keio collection. Mol Syst Biol 2:2006.0008.
563 55. Kinana AD, Vargiu A V., Nikaido H. 2013. Some ligands enhance the efflux of other

564 ligands by the escherichia coli multidrug pump AcrB. Biochemistry 52:8342–8351.
565 56. Hoeksema M, Jonker MJ, Brul S, Ter Kuile BH. 2019. Effects of a previously selected
566 antibiotic resistance on mutations acquired during development of a second resistance in
567 Escherichia coli. BMC Genomics 20:284.
568 57. Hirakawa H, Takumi-Kobayashi A, Theisen U, Hirata T, Nishino K, Yamaguchi A. 2008.
569 AcrS/EnvR represses expression of the acrAB multidrug efflux genes in Escherichia coli.
570 J Bacteriol 190:6276–6279.
571 58. Ray MJ, Tallman GB, Bearden DT, Elman MR, McGregor JC. 2019. Antibiotic
572 prescribing without documented indication in ambulatory care clinics: national cross
573 sectional study. BMJ 367:l6461.
574 59. Falagas ME, Makris GC, Dimopoulos G, Matthaiou DK. 2008. Heteroresistance: a
575 concern of increasing clinical significance? Clin Microbiol Infect 14:101–104.
576 60. Hennessy TW, Petersen KM, Bruden D, Parkinson AJ, Hurlburt D, Getty M, Schwartz B,
577 Butler JC. 2002. Changes in Antibiotic-Prescribing Practices and Carriage of Penicillin-
578 Resistant *Streptococcus pneumoniae*: A Controlled Intervention Trial in Rural Alaska.
579 Clin Infect Dis 34:1543–1550.
580 61. Čižman M. 2003. The use and resistance to antibiotics in the community. Int J Antimicrob
581 Agents 21(4):297–307.
582 62. Barbosa TM, Levy SB. 2000. Differential Expression of over 60 Chromosomal Genes in
583 Escherichia coli by Constitutive Expression of MarA. J Bacteriol 182:3467–3474.
584 63. Alekshun MN, Levy SB. 1999. The mar regulon: multiple resistance to antibiotics and
585 other toxic chemicals. Trends Microbiol 7.
586 64. Datta S, Costantino N, Court DL. 2006. A set of recombineering plasmids for gram-

587 negative bacteria. Gene 379:109–115.

588 65. Datsenko KA, Wanner BL. 2000. One-step inactivation of chromosomal genes in

589 *Escherichia coli* K-12 using PCR products. Proc Natl Acad Sci U S A 97:6640–6645.

590 66. Andrews JM. 2001. BSAC standardized disc susceptibility testing method. J Antimicrob

591 Chemother 48:43–57.

592 67. Kronvall G. 1982. Analysis of a single reference strain for determination of gentamicin

593 regression line constants and inhibition zone diameter breakpoints in quality control of

594 disk diffusion antibiotic susceptibility testing. J Clin Microbiol 16:784–793.

595 68. Deatherage DE, Barrick JE. 2014. Identification of mutations in laboratory-evolved

596 microbes from next-generation sequencing data using breseq. Methods Mol Biol

597 1151:165–188.

598

599

600 **FIGURE CAPTIONS**

601 **Figure 1. Evolution experiment schematic.** We used the eVOLVER, a modular turbidostat, as
602 an evolutionary platform to measure and record absorbance data at 600 nm (OD_{600}). We calculated
603 growth rate after each dilution event and collected samples at defined timepoints (t = 0, 1, 3, 6, 12,
604 24, 48, 72 h). We performed antibiotic disc assays and spot plate assays for all samples.

605

606 **Figure 2. Temporal landscapes based on treatment concentration of chloramphenicol. (A)**
607 Average growth rate. Growth rates are normalized to growth of strains at t = 0 h; for raw data see
608 Figure S1. Lighter areas represent growth rates closer to pre-treatment values; darker areas
609 represent reduced growth rates. MIC^0_{parent} concentration is denoted with a bold dashed line for
610 each strain (Figure S2). **(B)** Average resistance. Diameter of inhibition zones were plotted for each
611 time and treatment. Smaller inhibition zones are shown in red and correspond to resistant cells
612 (≤12 mm) and larger inhibition zones are shown in blue and represent susceptible cells (≥19 mm);
613 intermediate inhibition is shown with color scale from orange to green. MIC^0_{parent} is denoted with
614 a bold dashed line. **(C)** Final resistance at 72 h based on treatment concentration normalized to
615 MIC^0_{parent}. The final, absolute MIC is calculated based on data from Figure S5. Data points show
616 the mean of three biological replicates. Shaded error bars show standard deviation.

617

618 **Figure 3. Resistance and Fitness Evolution Trajectories. (A)** Average diameter of inhibition
619 zone and average growth rate plotted against each other. Lighter purple markers represent
620 trajectories occurring earlier; darker purple are later timepoints. The longer the distance between
621 markers, the greater the change between time points. Colors of boxes indicate the absolute
622 treatment concentration for the depicted trajectories. **(B)** Schematics summarize patterns for each

623 treatment concentration ($xMIC^0_{parent}$). Schematic plots show growth rate in terms of initial growth
624 rate (GR_0) and maximum physiological growth rate (GR_{max}). Resistance is shown in terms of
625 relative diameter of inhibition, where D_0 is the diameter of inhibition at t = 0 h and D_{min} is the
626 diameter of the antibiotic disc.
627
628 **Figure 4. Number of Biological Replicates with Highly Resistant Sub-populations through**
629 **Time.** Number of biological replicates that had a subpopulation greater than 0.1% of their total
630 population, which could grow on LB plates containing **(A)** 10 µg/mL or **(B)** 20 µg/mL
631 chloramphenicol. Raw data are shown in Figure S4. Initial populations contained ~10^7 CFUs.
632 MIC^0_{parent} is denoted with a bold dashed line.
633
634

635 **SUPPLEMENTARY FIGURE CAPTIONS**

636 **Figure S1. Growth rates for each biological replicate and antibiotic concentration.** Mean
637 growth rates for n = 3 biological replicates. Shaded error bars show standard deviation. Cultures
638 grown without chloramphenicol occasionally accumulated biofilms, leading to the large variations
639 in the growth measurements for the 0 μg/ml case.

640

641 **Figure S2. Toxicity curves for each parent strain.** Final OD_{600} was measured after 24 h (see
642 Methods: Determination of MIC). Data points show mean values from n = 3 biological replicates,
643 error bars show standard deviation.

644

645 **Figure S3. Inhibition zone diameters for each biological replicate and antibiotic**
646 **concentration.** Mean diameter of inhibition zones (D_{inh}) for n = 3 biological replicates. Shaded
647 error bars show standard deviation.

648

649 **Figure S4. Colony forming units (CFU) per mL counts for each treatment.** Mean CFU/mL
650 values from n = 3 biological replicates are shown, with error bars denoting standard deviation.

651

652 **Figure S5. Linear map between the natural log of the MIC and inhibition zone areas.** Data
653 are from inhibition zone diameters and MIC_{90} for each parent strains (e.g. AcrAB+) and the
654 evolved isolates of each parent strain from three different eVOLVER experiments (e.g. eAcrAB+1,
655 eAcrAB+2, and eAcrAB+3). MIC_{90} is defined as the point where OD_{600} is reduced to 10% of
656 normal growth after 24 h (Figure S2). To find the linear correlation, we calculated the natural log
657 of the MIC_{90} and the inhibition zone areas. The parameters for this map are Q = 30 μg, k = 57.8,

658 and K = -0.971, following the notation from Reference (67).

659

660 **Figure S6. Toxicity curves in the presence of Tween20.** Strains grown with and without 0.2%
661 (v/v) Tween20. Data points show mean values from n = 3 biological replicates, error bars show
662 standard deviation.

663

664 **SUPPLEMENTARY TABLE CAPTIONS**

665 **Table S1.** P-values from the (paired) *t*-test for quantifying significant differences in **(A)** growth
666 rate or **(B)** resistance as measured by the diameter of inhibition zone between (1) two sequential
667 time points, (2) a given time point and the initial time point, or (3) two strains at a given time point
668 and treatment.

669

670 **Table S2.** Summary of sequencing results. Non-clonal mutations for each resistant isolate from
671 eVOLVER experiments. Each isolate from each parent strain is derived from a different biological
672 replicate. In addition to the mutations, the table also lists the treatment concentrations that each
673 isolate evolved at, as well as the concentration of chloramphenicol that the isolate was selected on
674 at t = 72 h. Genetic regions that do not exist in the parent strain are grayed out.

675

676 **Table S3.** Primers containing 40-nt homology regions for *acrR* knockout. Bold letters denote the
677 active priming region to amplify pKD13 from Reference (54).

678

679 **Table S4.** P-values from the paired *t*-test to assess statistically significant differences in growth
680 between samples treated with Tween20 at 0.0% and 0.2% (v/v) as shown in Figure S6.

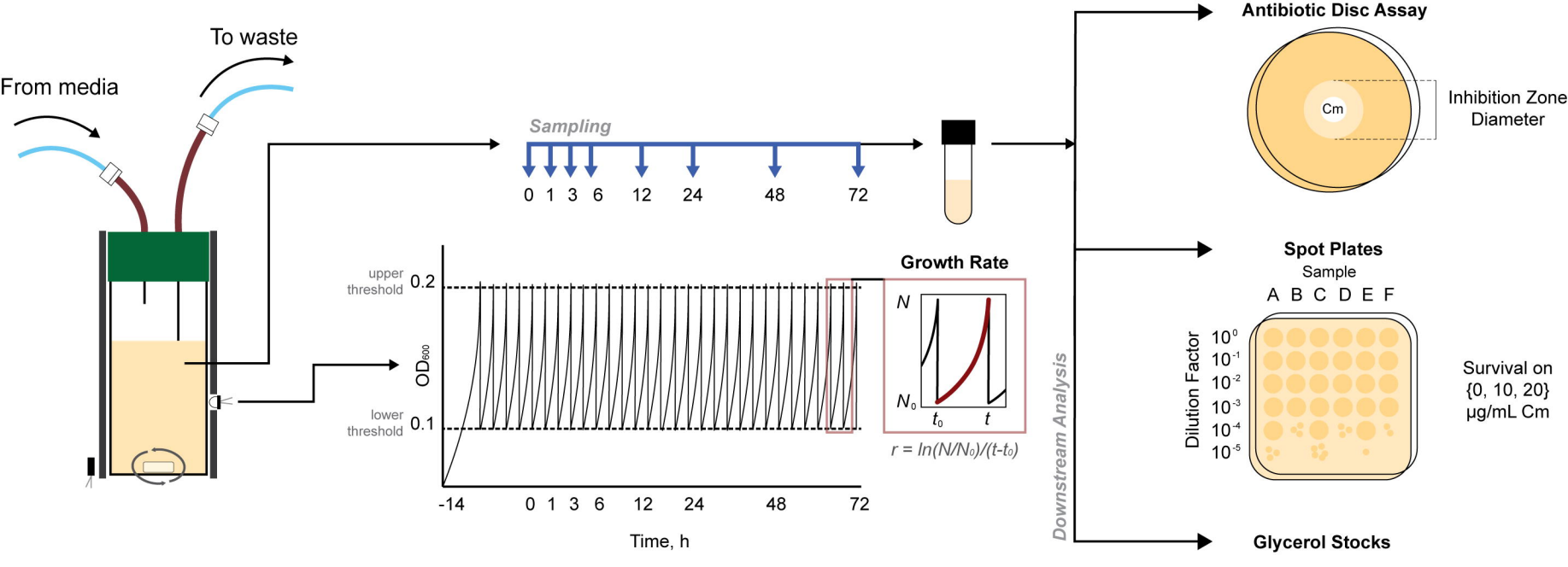
To waste
From media
Sampling
0 1 3 6 12 24 48 72
upper threshold
0.2
OD600
lower threshold
0.1
-14 0 1 3 6 12 24 48 72
Time, h
Growth Rate
N
N0
t0
t
r = ln(N/N0)/(t-t0)
Downstream Analysis
Antibiotic Disc Assay
Cm
Inhibition Zone Diameter
Spot Plates
Sample
A B C D E F
Dilution Factor
10^0
10^-1
10^-2
10^-3
10^-4
10^-5
Survival on {0, 10, 20} µg/mL Cm
Glycerol Stocks

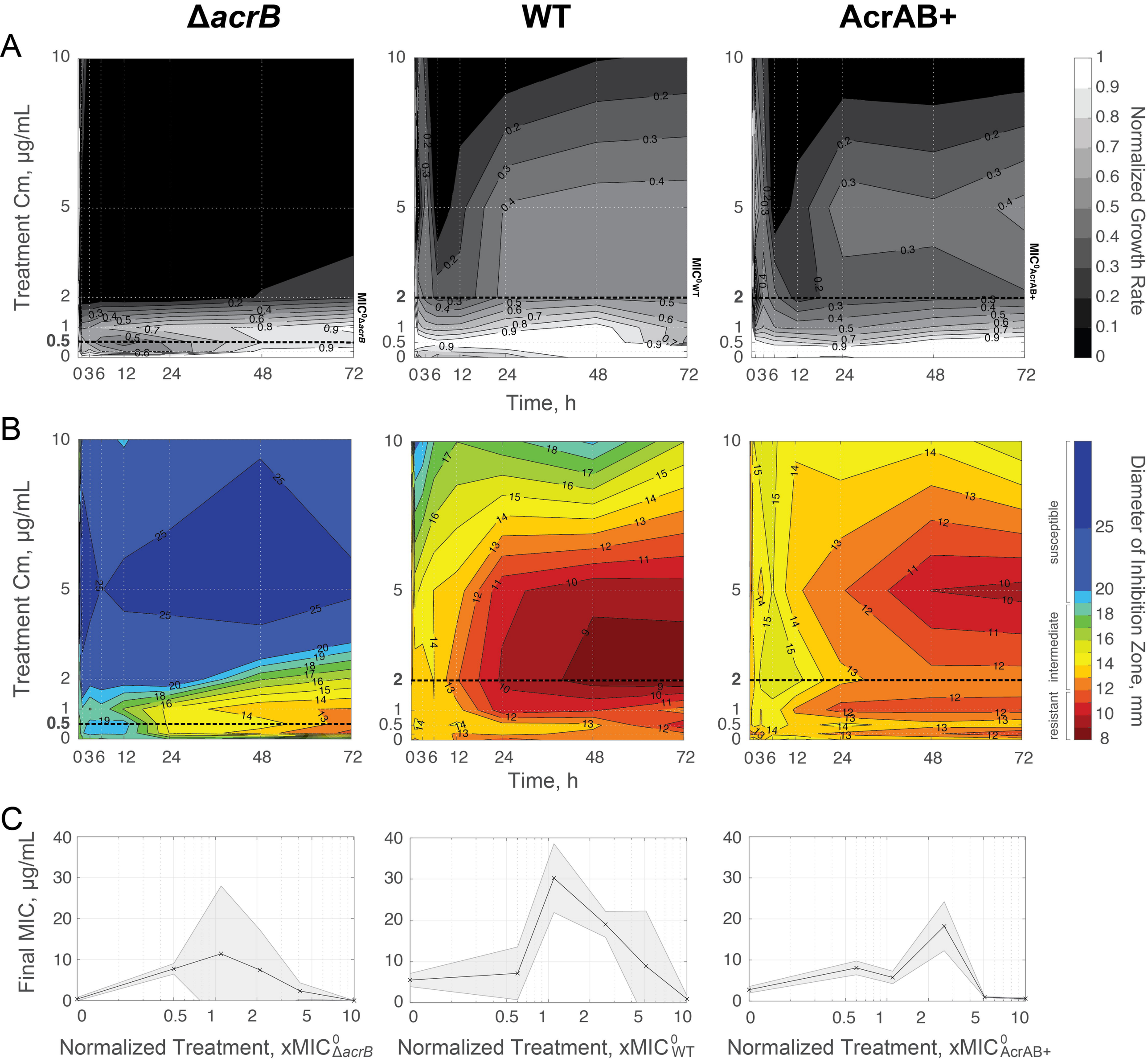
ΔacrB
WT
AcrAB+
A
Treatment Cm, μg/mL
Time, h
Normalized Growth Rate
MIC⁰ΔacrB
MIC⁰WT
MIC⁰AcrAB+
B
Treatment Cm, μg/mL
Time, h
Diameter of Inhibition Zone, mm
susceptible
intermediate
resistant
C
Final MIC, μg/mL
Normalized Treatment, xMIC⁰ΔacrB
Normalized Treatment, xMIC⁰WT
Normalized Treatment, xMIC⁰AcrAB+

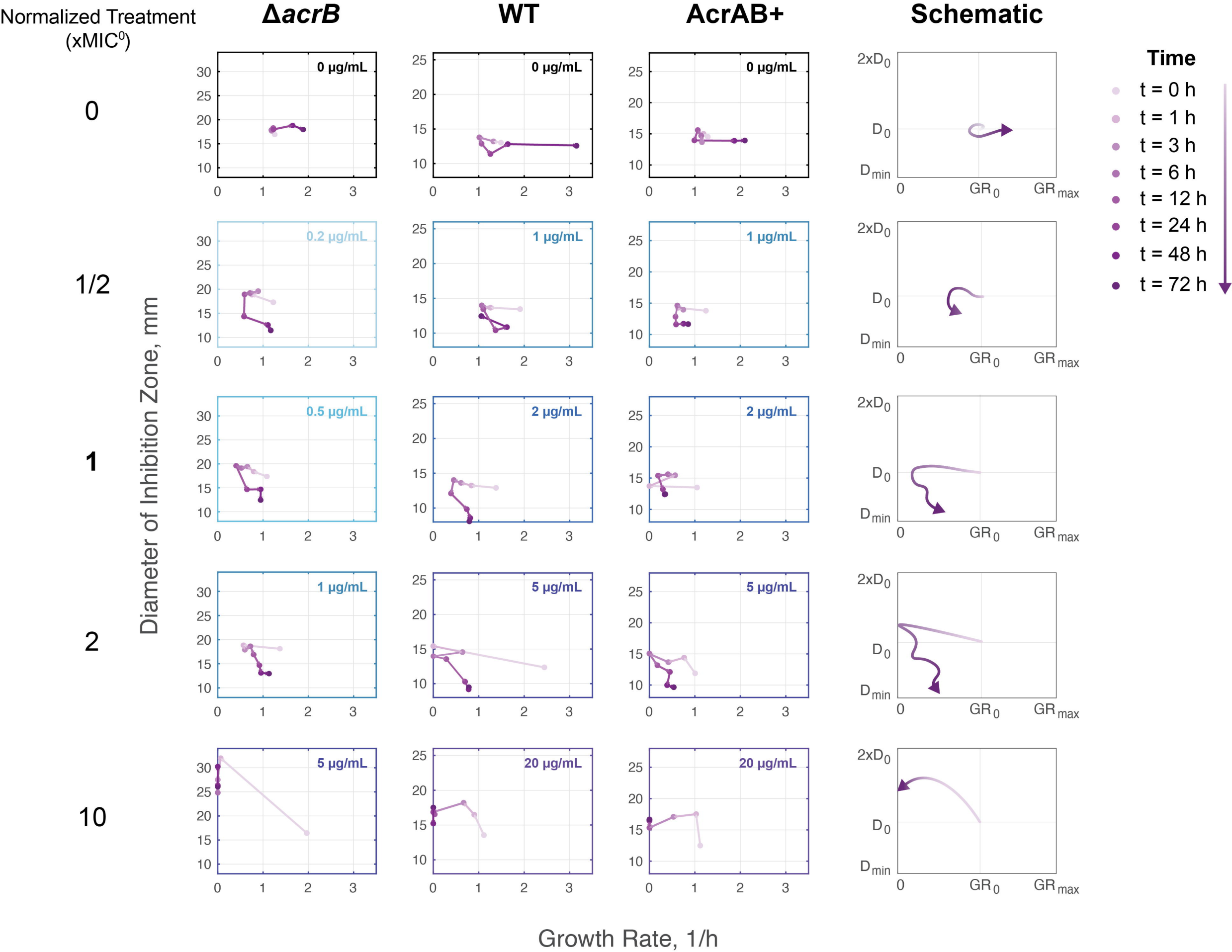
Normalized Treatment (xMIC⁰)
ΔacrB
WT
AcrAB+
Schematic
0
1/2
1
2
10
0 µg/mL
0.2 µg/mL
1 µg/mL
0.5 µg/mL
2 µg/mL
5 µg/mL
20 µg/mL
Diameter of Inhibition Zone, mm
Growth Rate, 1/h
2xD0
D0
Dmin
GR0
GRmax
Time
t = 0 h
t = 1 h
t = 3 h
t = 6 h
t = 12 h
t = 24 h
t = 48 h
t = 72 h

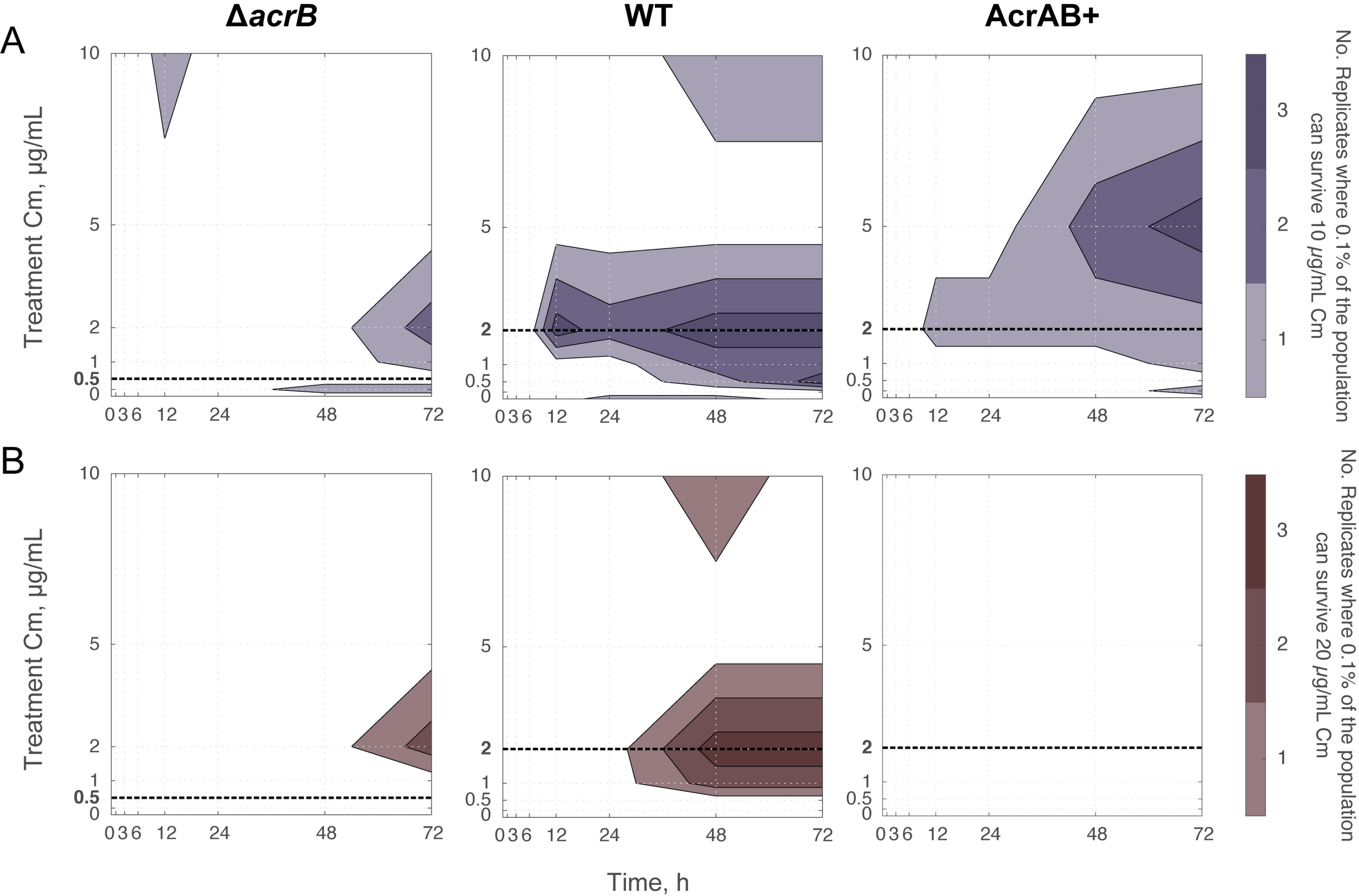
A
ΔacrB
WT
AcrAB+
Treatment Cm, µg/mL
10
5
2
1
0.5
0
0 3 6 12 24 48 72
No. Replicates where 0.1% of the population can survive 10 µg/mL Cm
3
2
1
B
Treatment Cm, µg/mL
No. Replicates where 0.1% of the population can survive 20 µg/mL Cm
Time, h